plete Γ functions[7] involving too many terms to be of practical use. It is also possible to find a series expansion in ϵ for these integrals by expanding the incomplete Γ function as a power series in ϵ. However, this expansion is only useful for relatively small ϵ.

Therefore, the integrals (B15) and (B16) are evaluated numerically. Romberg's quadrature procedure is used after the substitution $\cot an\theta = t$ is carried out. The integrand then satisfies the conditions to apply this procedure in an efficient manner. Good efficiency is required since the final result is a sum of 2×256 integrals of the type (B15) for every value of ϵ and α. For each (ϵ, α) point the numerical work takes about 10 min on an IBM 1130 computer.

In Appendix C some remarks are made concerning the accuracy of the results. The computer programs are given in Ref. 7.

APPENDIX C: COMPARISON OF SOME NUMERICAL PROCEDURES USED TO CALCULATE R

The integral S, occurring in the "special case" (see Sec. III), has been treated numerically in three different ways: (a) using the series (A5) and (A6) of Appendix A; (b) using the expressions (B15) and (B16) obtained for R and applying the numerical procedure described in Appendix B; (c) using Romberg's procedure for the direct calculation of the integral

$$\int_0^\infty x \frac{e^{-\epsilon x^2}}{1+x^2} \ln\left|\frac{1+x}{1-x}\right| dx .$$

This results in the information in Table I.

---

‡Present address: Physics Department, University of Antwerp (U.I.A), Fort VI-Straat, Wilryk 2610, Antwerp, Belgium.

*Work performed in the scope of the association R.U.C. Antwerpen–S.C.K./C.E.N., Mol, by the Theory of Nonmetallic Solids Team.

†Also at the Solid State Physics Department, S.C.K.–C.E.N., Mol, Belgium.

[1]E. Kartheuser, R. Evrard, and J. Devreese, Phys. Rev. Letters 22, 94 (1969).

[2]E. Kartheuser, R. Evrard, and J. Devreese, in *Optical Properties of Solids*, edited by E. D. Haidemenakis (Gordon and Breach, New York, 1970), Chap. XVIII.

[3]For a recent survey on polaron physics, see *Polarons in Ionic Crystals and Polar Semiconductors, Proceedings of the* 1971 *Antwerp Advanced Study Institute*, edited by J. Devreese (North-Holland, Amsterdam, 1972).

[4]J. C. Hermanson, Phys. Rev. 177, 1234 (1969).

[5]M. Goovaerts and J. Devreese, J. Math. Phys. (to be published).

[6]K. K. Bajaj, M. J. Goovaerts, and J. Devreese (unpublished).

[7]M. Goovaeris, J. De Sitter, and J. Devreese, Report No. BLG 439 (1969) (unpublished).

[8]C. C. Grosjean, Bull. Soc. Math. Belgium TXVII, 252 (1965).

[9]H. Willis, Phil. Mag. 455 (1946).

[10]In Ref. 7 it is shown that, in principle, (3.1) can be cast in analytical form. However, this leads to an unpractical result and therefore a numerical treatment is used here.

PHYSICAL REVIEW B VOLUME 7, NUMBER 6 15 MARCH 1973

Electronic Properties of Complex Crystalline and Amorphous Phases of Ge and Si. I. Density of States and Band Structures*

J. D. Joannopoulos and Marvin L. Cohen

Department of Physics, University of California, Berkeley, California 94720

Inorganic Materials Research Division, Lawrence Berkeley Laboratory, Berkeley, California 94720

(Received 15 September 1972)

We present calculations of the band structures and densities of states of Ge and Si in the diamond, wurzite, Si-III (BC-8), and Ge-III (ST-12) structures using the empirical-pseudopotential method and the tight-binding model used recently by Weaire. The increasing complexity of the crystal structures indicates that short-range disorder is able to account well for the density of states and optical properties of amorphous Ge and Si. This calculation also provides a method for explaining various features in the amorphous density of states and shows what structural aspects of the amorphous state are responsible for these features.

I. INTRODUCTION

The optical properties and density of states of amorphous Si and Ge obtained from experiment[1–4] exhibit some very interesting and sometimes novel features when compared with the corresponding ones of their crystalline phases. For example, the distinctive one-hump form of the imaginary

part of the dielectric function, $\epsilon_2(\omega)$, for amorphous Si and Ge has no counterpart in any known crystal except for the ST-12 structure in this calculation. For the density of states one finds experimentally the retention of a "gap" in the amorphous phase. This has been shown theoretically for some special models by Weaire and Thorpe[5] and McGill and Klima.[6] However, the conduction-band density of states seems to have none of the structure found in the crystalline phase [see Fig. 9(a)]. Furthermore, the form of the valence-band density of states in the amorphous phase consists of a smoothed blue-shifted peak at the top of the valence band and a seemingly large broad peak at the bottom of the valence band[3,4] (see Fig. 11). This is in contrast to the three strong peaks found in the valence bands of the crystalline phase.

Amorphous samples can be prepared in a variety of ways with a range in bulk density from 25% less to approximately the same as the bulk density of the crystalline case. There also exists a lot of speculation as to the structural nature of the amorphous phase. On this point there have been primarily two main schools of thought. First, the amorphous structure is made up of small domains of perfect crystals separated by disordered boundaries, which is called the "microcrystallite model." For example, Rudee and Howie[7] found that their amorphous films gave consistent diffraction-ring patterns with a microcrystallite model if their amorphous sample were made up of "wurtzite" microcrystals. Another approach is that the amorphous phase can exist in a completely disordered structure while each atom retains an imperfect tetrahedral arrangement of nearest neighbors. In this case if all the bonds are satisfied the model is called a "random-network model." Spicer and co-workers[1] seem to be able to prepare their amorphous samples in an "ideal" manner such that they have a negligible presence of microvoids and dangling bonds and have the same nearest-neighbor distance and approximately the same bulk density as that of the crystalline case. It is this type of sample that we will have in mind when we discuss and compare our results with the "amorphous phase."

It is clearly a formidable task to perform a realistic calculation on a structure with long-range disorder. However, we could ask the following question: How much disorder is necessary to achieve the distinctive features evident in the amorphous data? To explore the possible answers to this question, we have calculated the band structure and density of states for Ge and Si in the diamond, wurtzite, Si-III,[8] and Ge-III[8] structures using the empricial-pseudopotential method (EPM)[9] and the tight-binding model used recently by Weaire.[5] From the pseudopotential band structure we have also calculated the optical properties of these structures. The diamond structure is face-centered cubic with two atoms per primitive cell (FC-2), wurtzite is hexagonal 2H with four atoms per primitive cell (2H-4), Si III is body-centered cubic with eight atoms per primitive cell (BC-8), and Ge III is simple tetragonal with 12 atoms per primitive cell (ST-12). The Si-III and Ge-III structures are complicated dense metastable crystalline phases which are recovered from high-pressure experiments and persist at normal pressures. When Ge occurs in the Si-III structure it is called Ge IV.[10] Because of this rather unfortunate terminology we shall use the notation just described in parentheses for the specification of these various structures.

FC-2, 2H-4, BC-8, and ST-12 provide us with a series of structures that become more and more locally disordered. What we imply by local disorder is that we have a crystal (long-range order) and yet the atoms in the primitive cell of our crystal are in a "disordered" tetrahedral-like arrangement. The FC-2, 2H-4, and BC-8 structures are all similar in that they have sixfold rings of bonds and one type of atomic environment. The ST-12 structure, however, is very novel in that it has fivefold rings of bonds and two types of atomic environment. The electronic properties of these structures should then provide us with some interesting tests for the microcrystallite and random-network models and should provide us with an idea of how much disorder is necessary to reproduce the important features of the experimental amorphous data.

In this paper we shall concentrate on the band structure and density of states for the FC-2, 2H-4, BC-8, and ST-12 structures and we shall leave a detailed[11] discussion of the optical properties for a subsequent paper.

In Sec. II we shall give a description of these structures and the parameters that were used. In Sec. III we shall give a brief description of the calculations, and in Sec. IV we shall discuss our results. Finally, in Sec. V we shall make some concluding remarks.

II. STRUCTURE OF POLYTYPES AND THEIR PARAMETERS

Si has been found experimentally to exist in a 2H-4 structure by Wentorf and Kasper[12] with a 2% increase in density as compared to Si FC-2. The lattice constants they obtained were $a = 3.80$ Å and $c = 6.28$ Å. In our calculations we assume, in addition, an ideal $u = 0.375$. Ge, on the other hand, has not yet been found, to our knowledge, to exist in a hexagonal structure so that we assumed an ideal Ge 2H-4 with the same density and nearest-neighbor distance (2.45 Å) as that of Ge FC-2.

Si and Ge have both been found to exist in the BC-8 [10,12] structure which can be specific completely by a lattice constant a and an internal parameter x. The lattice constant for Si is $a = 6.636$ Å and for Ge we have $a = 6.92$ Å. The internal parameter x was taken to be $x = 0.1$. Each linked pair of Si (Ge) atoms has one bond length 2.30 Å (2.40 Å) and three bonds of length 2.40 Å (2.50 Å), with an average bond length approximately equal to 2.37 Å (2.48 Å). There are also two types of bond angles approximately equal to 118° and 100° for both Ge and Si. All the eight atoms in the primitive cell are of one type in that they exist in the same type of environment with the same relative arrangement of neighboring atoms. For Si (Ge) there is one next-nearest neighbor at 3.45 Å (3.60 Å), six at 3.57 Å (3.73 Å), six at 3.87 Å (4.04 Å), etc.

Ge has been found to exist in the ST-12 structure whereas Si has not. The ST-12 structure is specified by two lattice constants a, c and four internal parameters x_1, x_2, x_3, and x_4. For Ge (Si) we used $a = 5.93$ Å (5.69 Å) and $c = 6.98$ Å (6.70 Å). The Si lattice constants were chosen so that the c/a ratio is the same as that of Ge ST-12 and the fractional density change from Si FC-2 to Si ST-12 is the same as Ge FC-2 to Ge ST-12. For Ge and Si the internal parameters were taken to be $x_1 = 0.09$, $x_2 = 0.173$, $x_3 = 0.378$, and $x_4 = 0.25$. In this structure the bond lengths are all about the same length and approximately equal to 2.49 Å (2.39 Å) for Ge (Si). The bond angles, however, are quite dissimilar. They range from 20% less to 25% greater than the ideal tetrahedral angle (109°28′). In this structure the Ge or Si atoms are positioned in two different types of environment. In the primitive cell there are four atoms of type 1 and eight atoms of type 2. The atoms of type 2 form long fourfold spiral chains along the $\vec{c}$ direction while atoms of type 1 form bonds between atoms in the different spirals. For Ge, atoms of type 1 have two next-nearest neighbors at 3.45 Å, two at 3.64 Å, two at 3.81 Å, etc. Kasper and Richards[8] neglected to mention the presence of the first two pairs of next-nearest neighbors. Atoms of type 2 for Ge ST-12 have one next-nearest neighbor at 3.45 Å, two at 3.56 Å, one at 3.64 Å, etc. Finally, the ST-12 structure is quite unusual because of the presence of fivefold rings of bonds.

It is evident that Ge ST-12 and Si ST-12 have many of the properties one would intuitively attribute to an "ideal" amorphous structure. That is, (i) no dangling bonds, (ii) variations in bond length and angle, (iii) atoms in different environments, and (iv) the occurrence of five numbered rings of bonds. On the other hand, Ge and Si in the BC-8 structure are more closely associated with the 2H-4 and FC-2 structures since they have even numbered rings of bonds and only one type of atomic environment.

The bulk densities of Ge ST-12 (Si ST-12) and Ge BC-8 (Si BC-8) differ by about 1%. However, they are both about 10% greater than those of Ge FC-2 (Si FC-2) and certain types of amorphous Ge (Si).[1] Therefore a comparison of the differences between the optical properties and density of states of Ge FC-2 (Si FC-2) and Ge BC-8 (Si BC-8) can be attributed primarily to structural and symmetry differences. Hence comparisons of the polytypes provide a method of filtering out the effects of greater density which should be small since the nearest-neighbor distances in the ST-12 and BC-8 structures are slightly larger than those in the FC-2 and 2H-4 structures.

Since we have been discussing the structural aspects of the ST-12 structure we would like to mention that we were able to build a crystal with the same symmetry and number of atoms in the primitive cell as Ge ST-12 but with the same nearest-neighbor distance and bulk density as amorphous Ge. The method consisted of finding three independent bond lengths b_1, b_2, b_3 which were functions of a, x_1, x_2, x_3, x_4, and V such that $c = V/a^2$. Once the density was fixed through V we minimized the function

$$M(x_1, x_2, x_3, x_4, a) = \sum_{i=1}^{3} [b_i(x_1, x_2, x_3, x_4, a) - l_i]^2, \quad (1)$$

where the l_i are the bond lengths desired, by a method of steepest descent. Although we obtained the correct bond lengths and bulk density, and a good radial distribution function, we obtained some bond angles that were 40% larger than the ideal tetrahedral angle. These large deviations in our modified crystal produced large deviations in the Hamiltonian matrix elements and we found that we obtained a semimetal. This is in large contrast to the fact that we found quite a sizable gap for Ge ST-12. This will be of interest later when we discuss what structural aspects affect the size of the energy gap.

III. CALCULATIONS

The empirical-pseudopotential method has been discussed extensively in an article by Cohen and Heine.[9] The EPM essentially entails removing the large potential of the core along with the many oscillations of the wave functions in the core. The valence pseudo-wave-function $\psi_{\vec{k}}(\vec{r})$ is then in essence the true valence wave function minus the core states and satisfies the Schrödinger equation

$$[p^2/2m + V(\vec{r})]\,\psi_{\vec{k}}(\vec{r}) = E(\vec{k})\,\psi_{\vec{k}}(\vec{r}), \quad (2)$$

where $V(\vec{r})$ is the pseudopotential and the $E(\vec{k})$ are the eigenvalues of the real valence-electron wave functions. The weak periodic pseudopotential $V(\vec{r})$ can now be expanded in a small number of plane waves:

$$V(\vec{r}) = \sum_{\vec{G}} V(\vec{G}) e^{i\vec{G}\cdot\vec{r}} \quad \text{for} \quad |\vec{G}| \leq |\vec{G}_0|, \tag{3}$$

where $|\vec{G}_0|$ represents some cutoff reciprocal-lattice vector. For the case of one type of atom $V(\vec{G})$ can be written

$$V(\vec{G}) = V_f(\vec{G}) S(\vec{G}), \tag{4}$$

where $S(\vec{G})$ is the structure factor and $V_f(\vec{G})$ is a form factor of the atomic potential which is fitted to experimental optical data. $S(\vec{G})$ and $V_f(\vec{G})$ are given by

$$S(\vec{G}) = \frac{1}{n} \sum_i e^{-i\vec{G}\cdot\vec{\tau}_i}, \tag{5}$$

$$V_f(\vec{G}) = \frac{n}{\Omega} \int V_a(\vec{r}) e^{-i\vec{G}\cdot\vec{r}} d^3r, \tag{6}$$

where n is the number of atoms per primitive cell, $\vec{\tau}_i$ is the position of the ith atom in the primitive cell, Ω is the volume of the primitive cell, and $V_a(\vec{r})$ is the atomic potential. If we assume a spherical atomic potential then $V_f(\vec{G})$ depends only on the magnitude of $\vec{G}$. For Si and Ge in the FC-2 structure, Cohen and Bergstresser[13] used only three form factors to obtain a good agreement of calculated optical properties with experiment. Once one has a good set of form factors, the atomic-pseudopotential form factors can be obtained from Eq. (6). If one now assumes the atomic potentials do not change very much from one type of crystal structure to the next, the form factors can be used for a variety of crystalline structures. In this sense the EPM is extremely useful. The procedure essentially involves obtaining a continuous $V_f(|\vec{q}|)$ by a suitable interpolation scheme and reading off the $V_f(|\vec{G}|)$ for the set of $\vec{G}$ spanning the reciprocal lattice of the particular polytype structure. The first calculation of this type was done by Bergstresser and Cohen[14] for CdSe, CdS, and ZnS in the 2H-4 structure.

Since no experimental data are available at this time for the polytypes we have studied, the form factors we have obtained might have to be adjusted slightly to give better agreement with experiment. In Tables I and II we list the unnormalized form factors for Ge and Si and the corresponding reciprocal-lattice vectors for the 2H-4, BC-8, and ST-12 crystal structures. For the 2H-4 structure we used 50–60 plane waves as a basis set along with another 140 plane waves through a perturba-

TABLE I. Reciprocal-lattice vectors, their magnitudes, and form factors for Ge in the 2H-4, BC-8, and ST-12 structures. The reciprocal-lattice vectors are expressed with respect to the primitive translation vectors for each structure and the magnitudes of these vectors are in units of $(2\pi/a_0)^2$, where a_0 is the lattice constant for Ge in the FC-2 structure. The form factors are in Ry and should be multiplied by a factor equal to the ratio of bulk density of the particular Ge structure to the Ge FC-2 structure. Some of the form factors of Ge 2H-4 are omitted since the structure factors are zero for these $\vec{G}$'s.

	Ge 2H-4			Ge BC-8			Ge ST-12				
$\vec{G}$	G^2	V_f	$\vec{G}$	G^2	V_f	$\vec{G}$	G^2	V_f	$\vec{G}$	G^2	V_f
(0,0,1)	0.750	···	(1,0,0)	1.338	−0.380	(0,0,1)	0.658	−0.470	(3,1,0)	9.110	0.040
(1,0,0)	2.667	−0.255	(1,1,−1)	2.676	−0.255	(1,0,0)	0.911	−0.435	(2,0,3)	9.562	0.048
(0,0,2)	3.000	−0.230	(1,1,0)	4.014	−0.165	(1,0,1)	1.569	−0.350	(3,1,1)	9.768	0.050
(1,0,1)	3.417	−0.200	(2,0,0)	5.352	−0.093	(1,1,0)	1.822	−0.325	(2,2,2)	9.918	0.053
(1,0,2)	5.667	−0.075	(2,1,−1)	6.690	−0.035	(1,1,1)	2.480	−0.270	(2,1,3)	10.473	0.060
(0,0,3)	6.750	···	(1,1,1)	8.028	−0.010	(0,0,2)	2.630	−0.258	(0,0,4)	10.521	0.060
(1,1,0)	8.000	0.010	(2,1,0)	9.366	0.045	(1,0,2)	3.541	−0.193	(3,0,2)	10.829	0.060
(1,1,1)	8.750	···	(2,2,−2)	10.704	0.060	(2,0,0)	3.644	−0.188	(1,0,4)	11.432	0.060
(1,0,3)	9.417	0.045	(3,0,0)	12.042	0.053	(2,0,1)	4.302	−0.148	(3,1,2)	11.740	0.055
(2,0,0)	10.667	0.060	(3,1,−1)	13.380	0.038	(1,1,2)	4.522	−0.140	(3,2,0)	11.843	0.055
(1,1,2)	11.000	0.060	(2,1,1)	14.718	0.018	(2,1,0)	4.555	−0.135	(1,1,4)	12.343	0.050
(2,0,1)	11.417	0.060				(2,1,1)	5.213	−0.098	(3,2,1)	12.501	0.048
(0,0,4)	12.000					(0,0,3)	5.918	−0.065	(2,2,3)	13.206	0.040
(2,0,2)	13.667	0.035				(2,0,2)	6.274	−0.050	(3,0,3)	14.117	0.025
(1,0,4)	14.667					(1,0,3)	6.829	−0.030	(2,0,4)	14.165	0.025
(1,1,3)	14.750					(2,1,2)	7.185	−0.018	(3,2,2)	14.473	0.023
						(2,2,0)	7.288	−0.013	(4,0,0)	14.576	0.020
						(1,1,3)	7.740	0.003	(3,1,3)	15.028	0.013
						(2,2,1)	7.946	0.010	(2,1,4)	15.076	0.013
						(3,0,0)	8.199	0.018	(4,0,1)	15.234	0.010
						(3,0,1)	8.857	0.035	(4,1,0)	15.487	0.008

TABLE II. Reciprocal-lattice vectors, their magnitudes, and form factors for Si in the 2H-4, BC-8, and ST-12 structures. The convention is the same as Table I.

Si 2H-4			Si BC-8			Si ST-12					
$\vec{G}$	G^2	V_f	$\vec{G}$	G^2	V_f	$\vec{G}$	G^2	V_f	$\vec{G}$	G^2	V_f
(0,0,1)	0.748	−0.510	(1,0,0)	1.339	−0.420	(0,0,1)	0.658	−0.520	(3,1,0)	9.110	0.068
(1,0,0)	2.723	−0.245	(1,1,−1)	2.678	−0.250	(1,0,0)	0.911	−0.480	(2,0,3)	9.562	0.073
(0,0,2)	2.991	−0.210	(1,1,0)	4.017	−0.120	(1,0,1)	1.569	−0.380	(3,1,1)	9.768	0.075
(1,0,1)	3.470	−0.165	(2,0,0)	5.356	−0.050	(1,1,0)	1.822	−0.350	(2,2,2)	9.918	0.078
(1,0,2)	5.713	−0.035	(2,1,−1)	6.696	−0.001	(1,1,1)	2.480	−0.270	(2,1,3)	10.473	0.080
(0,0,3)	6.729	0.001	(1,1,1)	8.035	0.041	(0,0,2)	2.630	−0.255	(0,0,4)	10.521	0.080
(1,1,0)	8.168	0.045	(2,1,0)	9.374	0.070	(1,0,2)	3.541	−0.160	(3,0,2)	10.829	0.080
(1,1,1)	8.915	0.063	(2,2,−2)	10.713	0.080	(2,0,0)	3.644	−0.153	(1,0,4)	11.432	0.080
(1,0,3)	9.451	0.073	(3,0,0)	12.052	0.078	(2,0,1)	4.302	−0.105	(3,1,2)	11.740	0.078
(2,0,0)	10.890	0.080	(3,1,−1)	13.391	0.065	(1,1,2)	4.522	−0.093	(3,2,0)	11.843	0.078
(1,1,2)	11.158	0.080	(2,1,1)	14.730	0.040	(2,1,0)	4.555	−0.090	(1,1,4)	12.343	0.075
(2,0,1)	11.638	0.079				(2,1,1)	5.213	−0.058	(3,2,1)	12.501	0.075
(0,0,4)	11.962	0.078				(0,0,3)	5.918	−0.030	(2,2,3)	13.206	0.068
(2,0,2)	13.881	0.058				(2,0,2)	6.274	−0.015	(3,0,3)	14.117	0.055
(1,0,4)	14.684	0.040				(1,0,3)	6.829	0.005	(2,0,4)	14.165	0.054
(1,1,3)	14.896	0.035				(2,1,2)	7.185	0.015	(3,2,2)	14.473	0.047
						(2,2,0)	7.288	0.020	(4,0,0)	14.576	0.045
						(1,1,3)	7.740	0.033	(3,1,3)	15.028	0.030
						(2,2,1)	7.946	0.040	(2,1,4)	15.076	0.030
						(3,0,0)	8.199	0.045	(4,0,1)	15.234	0.025
						(3,0,1)	8.857	0.063	(4,1,0)	15.487	0.015

tion scheme developed by Löwdin.[15] We calculated $E(\vec{k})$ in $\frac{1}{24}$ of the Brillouin zone at 275 grid points. For the BC-8 structure we used approximately 60–65 plane waves as a basis with about 160 additional plane waves through perturbation theory. We diagonalized our Hamiltonian in $\frac{1}{48}$ of the Brillouin zone at 240 grid points. Finally, for ST-12 we used about 70 plane waves as a basis set along with approximately 270 more plane waves through the Löwdin scheme. The eigenvalues were obtained in $\frac{1}{16}$ of the Brillouin zone at 251 grid points. For all these structures we obtain a convergence of ≤ 0.1 eV for almost all the states in valence band and for the states in the conduction band in the vicinity of the gap.

In our tight-binding calculation we took the model used recently by Weaire and Thorpe.[5] The Bloch wave functions for each band have the form

$$\psi_{\vec{k},n}(\vec{r}) = \sum_{m=1}^{M} C_m^n X_{\vec{k},m}(\vec{r}), \tag{7}$$

where the $X_{\vec{k},m}(\vec{r})$ form a basis set of order M of tight-binding Bloch states given by

$$X_{\vec{k},m}(\vec{r}) = N^{-1/2} \sum_{\vec{R}} e^{i\vec{k}\cdot\vec{R}} \varphi(\vec{r} - \vec{R} - \vec{\tau}_i - \vec{\rho}_l), \tag{8}$$

where $m \equiv i, l$; N is the number of primitive cells and the φ_m are localized orthonormal states which can be taken as (sp^3) hybridized directed orbitals (four to each atom). The position of the ith atom in the primitive cell is given by $\vec{\tau}_i$, and $\vec{\rho}_l$ designates the direction and center-of-mass position of the lth directed orbital of the ith atom. Furthermore, for $i \neq i'$, $l' = l$ will imply that $-\vec{\rho}_l = \vec{\rho}_{l'}$ and that $|\vec{\tau}_i - \vec{\tau}_{i'}|$ is equal to a bond length. Thus states $\varphi_{i',l}$ and $\varphi_{i,l}$ are orbitals from different atoms which lie in the same bond and $\varphi_{i,l}$ and $\varphi_{i,l'}$ represent different orbitals defined with respect to the same atom.

In this model there are only two important nonzero matrix elements given by

$$\langle i, l | H | i, l' \rangle = V_1 \quad \text{and} \quad \langle i, l | H | i', l \rangle = V_2 . \tag{9}$$

The parameters V_1 and V_2 for the FC-2 structure were obtained by fitting them to the valence-band density of states of Ge FC-2 using the EPM. The values obtained were $V_1 = -2.22$ and $V_2 = -6.20$ and were taken to be the same for the BC-8 and ST-12 structures. The Weaire model of course assumes all the bond lengths are equal and a perfect tetrahedral arrangement for the atoms. The most prominent features of this model are a flat band at the top of the valence band containing two states per atom, a rather inadequate conduction band due to the limited number of basis functions, and an energy gap which is the same for all structures with even-numbered rings of bonds.

Once the band structure is known the density of states can be obtained using the following expression:

$$N(E) = \frac{1}{NN_a} \sum_{\vec{k}} \sum_{n} \delta(E - E_n(\vec{k})), \tag{10}$$

where N_a is the number of atoms in the primitive

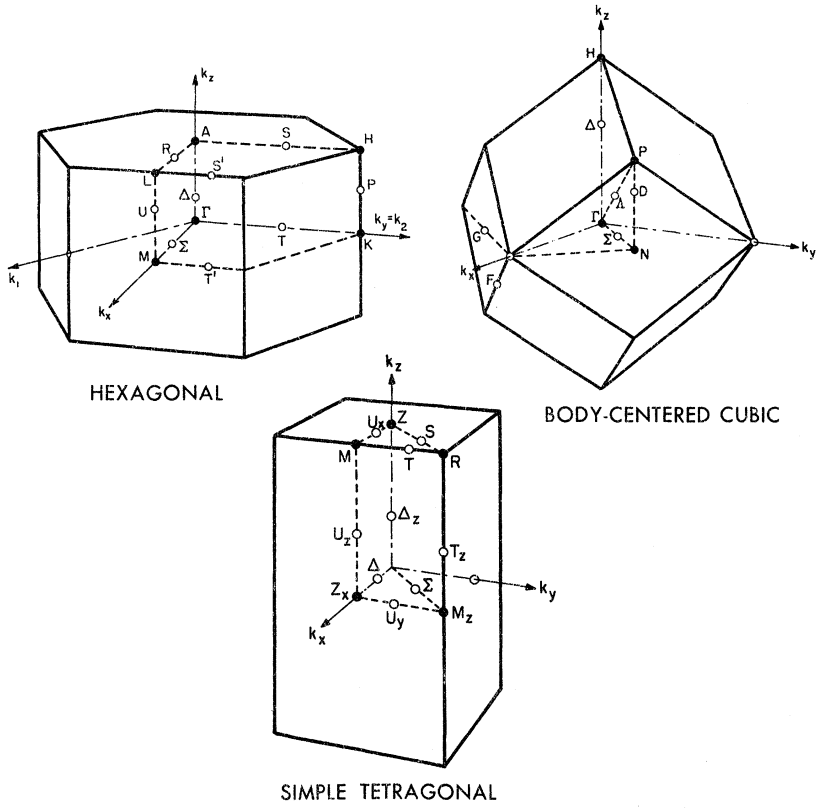

FIG. 1. Brillouin zones and associated symmetry points and lines for the 2H-4, BC-8, and ST-12 structures.

cell, N is the number of primitive cells, and $N(E)$ is normalized to the number of states per atom. The method used to evaluate the integral in Eq. (10) is due to Gilat and Raubenheimer.[16] The energy derivatives required by this method were obtained using $\vec{k}\cdot\vec{p}$ perturbation theory.

IV. RESULTS

In Fig. 1 we show the Brillouin zones for the 2H-4, BC-8, and ST-12 structures and the symmetry notation used by Leuhrmann.[17] The band structures of Ge and Si in these structures are

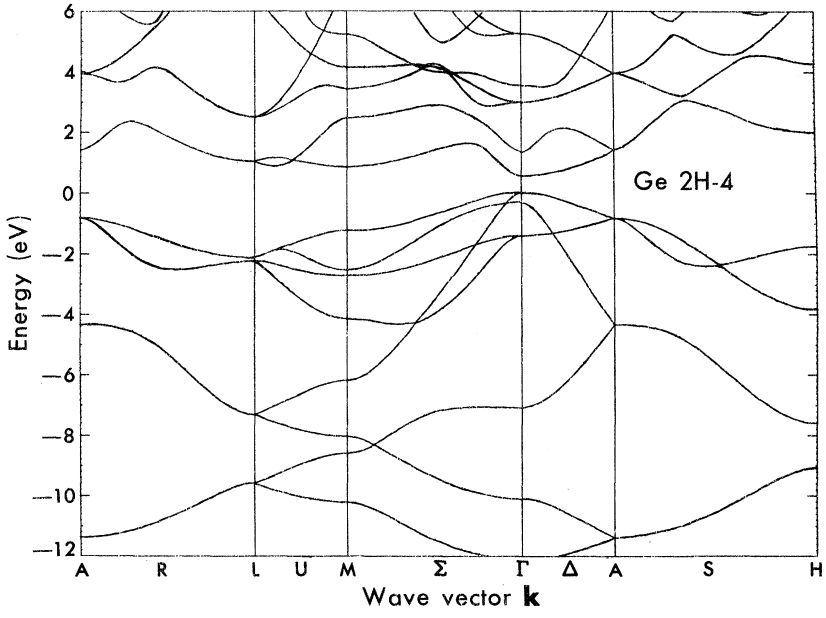

FIG. 2. Band structure of Ge in the 2H-4 or wurtzite structure.

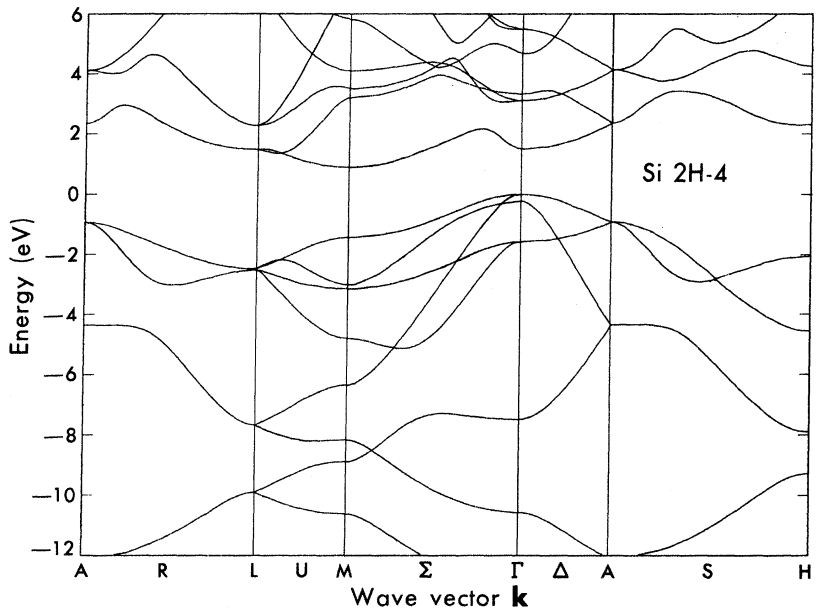

FIG. 3. Band structure of Si in the 2H-4 or wurtzite structure.

shown in Figs. 2–7.

Certain symmetry directions in the 2H-4 structure can be compared with analogous ones in the FC-2 structure through an alignment of the Brillouin zones.[14,18] One finds that the ΓL direction (FC-2) maps into the $\Gamma A \Gamma$ direction (2H-4) so that the indirect gap at L for Ge FC-2 becomes a direct gap at Γ in Ge 2H-4 and is equal to 0.55 eV. Although the ΓX direction (FC-2) is not associated with any symmetry direction in 2H-4, the X point is found to lie $\frac{2}{3}$ along the U axis from M to L (2H-4). Si, however, which has an indirect gap at X in the FC-2 structure, has an indirect gap at M in the 2H-4 structure equal to 0.85 eV.

In the BC-8 structure we find direct gaps for Si and Ge and they both occur at H. For Ge we obtain a zero gap whereas for Si we obtain 0.43 eV. It is interesting that in the Weaire BC-8 band structure we find the bottom of the conduction band also occurs at H.

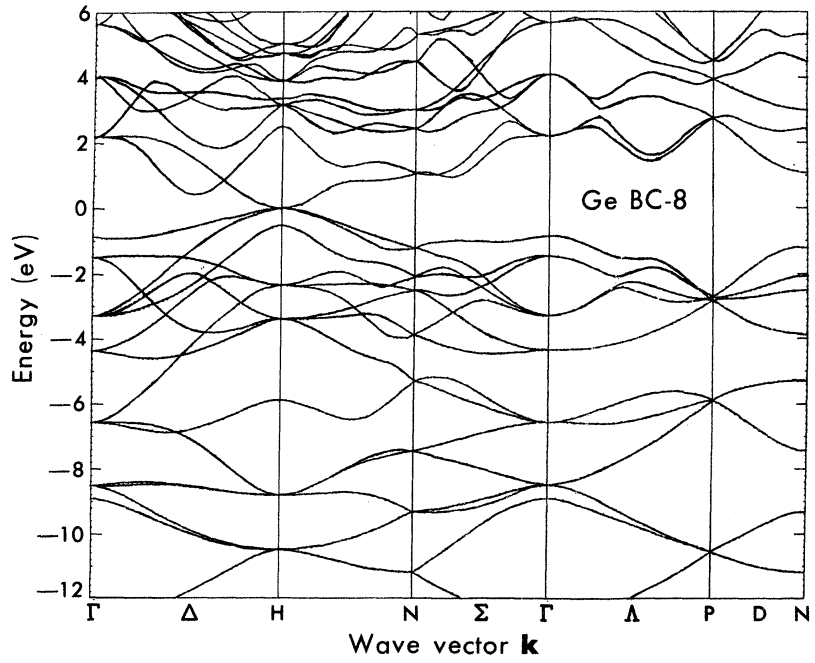

FIG. 4. Band structure of Ge in the BC-8 or Si III structure.

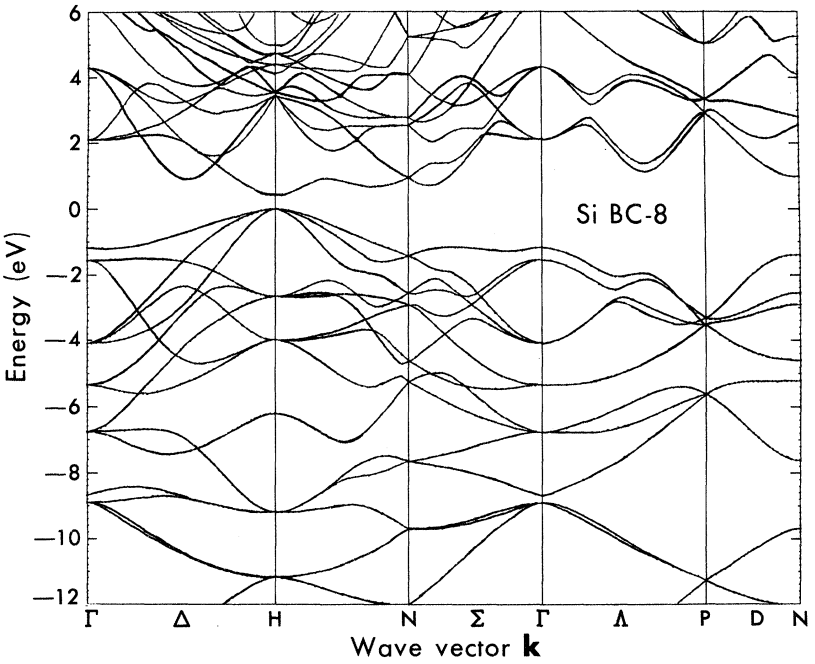

FIG. 5. Band structure of Si in the BC-8 or Si III structure.

In the ST-12 structure we find a direct gap for Ge 0.7 of the way from Γ to M_z. The magnitude of the gap is 1.47 eV. For Si we obtain an indirect gap with the top of the valence band 0.4 of the way from Γ to M_z and the bottom of the conduction band about 0.75 of the way between Γ and Z_x. The Si gap is equal to 1.6 eV. It should be mentioned, however, that since the valence band is rather flat along many symmetry directions and the conduction band has many dips at very nearly the same energy, the actual experimental gap could be direct or indirect and could lie in a variety of places. It is interesting, nevertheless, that we find using the Weaire tight-binding model that the ST-12 gap lies at M_z.

What is striking in this calculation is that the Ge and Si ST-12 gaps are about 50% larger than those of all the other structures. This is probably due to the influence of the large numbers of fivefold, and sevenfold rings in the ST-12 structure which would prevent the presence of low-lying antibonding s-like states in the conduction band. Weaire and Thorpe have suggested this might happen in structures with odd-numbered rings, but the degree to which it happens is shown in Fig. 8. Here we show the results of our calculation on an "ideal"

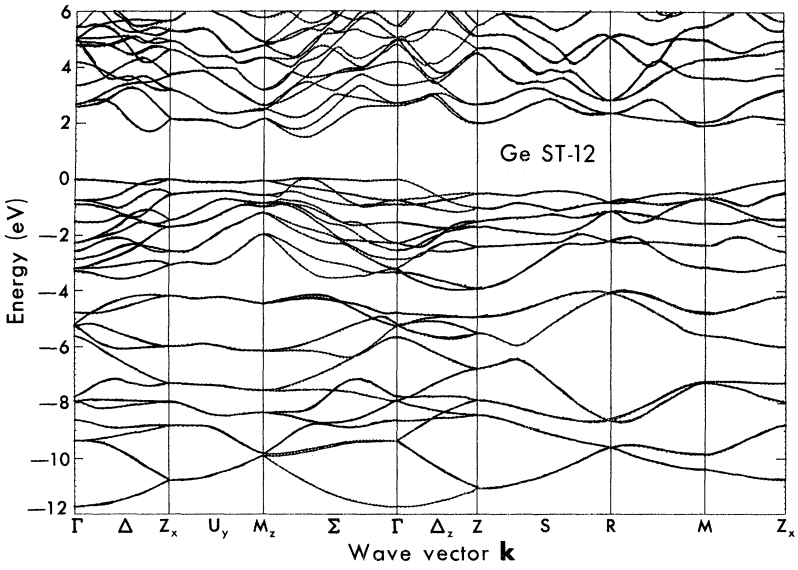

FIG. 6. Band structure of Ge in the ST-12 or Ge III structure.

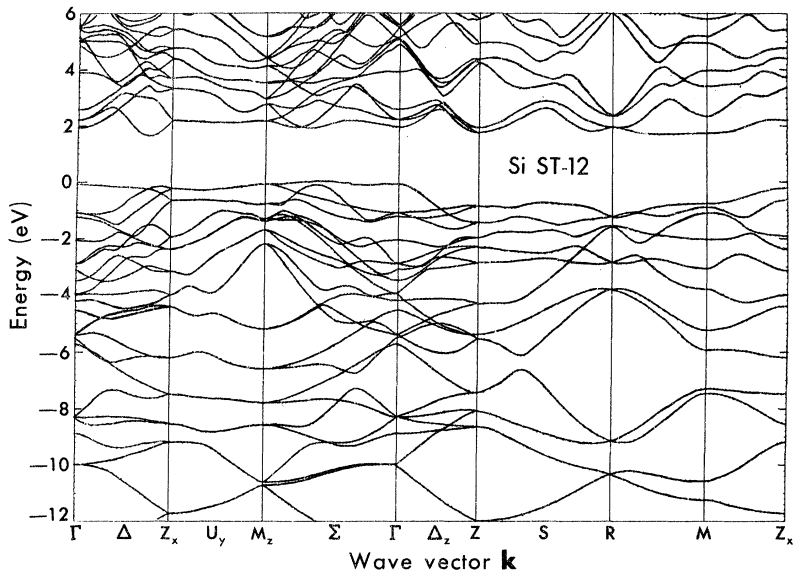

FIG. 7. Band structure of Si in the ST-12 or Ge III structure.

ST-12 and BC-8 structure using the Weaire model. At the top of the valence band we have the p-like δ-function peak containing two states per atom, while the rest of the valence band is s like and also contains two states per atom. We notice in Fig. 8(b) that we now have a "valence gap" and a "conduction gap." The conduction gap for ST-12 is considerably larger than that of BC-8 and FC-2 (dot-

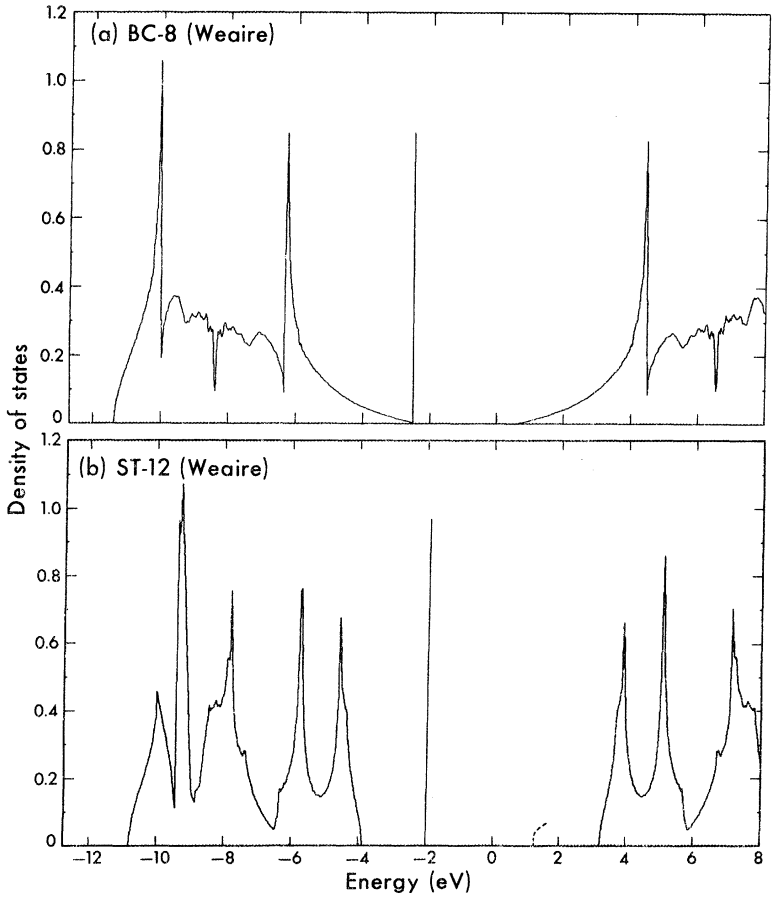

FIG. 8. Density of states for the (a) BC-8 and (b) ST-12 structures calculated from the tight-binding model used by Weaire. The BC-8 structure is shifted slightly to lower energies with respect to the ST-12 structure so as to agree better with Ge BC-8 (EPM). The dotted line in (b) represents the bottom of the conduction band for the FC-2 structure using the Weaire model.

ted line). In fact, we find a 200% increase in the gap if we include an *ad hoc* 2.0-eV broadening of the δ-function peak at the top of the valence band. In this model the valence and conduction gaps are intimately related. This is because the conduction- and valence-band eigenvalues (except for the pure p-like states) are associated through the same analytic transformation (aside from a sign) to the eigenvalues of a one-state Hamiltonian.[19] The coefficient of a one-state wave function is then equal to the sum of the coefficients of the corresponding four states in the old Hamiltonian which is just the s coefficient of these four states. Thus the omission of antibonding states in the one-state Hamiltonian will reflect itself in the omission of s-like states from the top of the valence band and bottom of the conduction band.

In the EPM case we do not expect such large effects since we obtain a much more realistic band structure. Nevertheless, the low-energy conduction-band states are rather localized and so we still expect the influence of odd-membered rings to be important. In fact, we can even observe a valence gap in Figs. 6 and 7 for Ge ST-12 and Si ST-12. In Ge ST-12 the s- and p-like states are almost separated while in Si ST-12 there is just a little mixing around -4.4 eV.

In Figs. 9(a)–9(d) we show plots of the density of states for Ge in the FC-2, 2H-4, BC-8, and ST-12 structures. Similar results for Si are shown in Fig. 10. Superimposed on the Ge (Si) FC-2 density of states is a sketch of the amorphous density of states obtained by Donovan and Spicer[1] (Pierce and Spicer[2]). The sharp peaks are primarily due to Bragg gaps[20] and would be smoothed out in a structure with no periodicity. Keeping this in mind we can make some interesting comparisons among these structures and we can examine the trends in going from FC-2 to 2H-4, to BC-8, to ST-12, to amorphous.

First we notice that the conduction band becomes more and more smoothed out as we go from FC-2 to ST-12. This lack of large structure also seems to be evident in the amorphous phase. Next we notice that the two large peaks at the bottom of the valence band in FC-2 seem to gain more structure as we go to 2H-4 and BC-8. Nevertheless, these peaks still retain most of their individual identity. In the ST-12 structure, however, there is a thorough mixing of the two peaks. This is similar to the suggestion by Thorpe and Weaire[21] for the amorphous case. Experimentally, Wiech and Zöpf[3] did find a seemingly large broad peak at the bottom of the valence band for amorphous Si using soft-x-ray spectroscopy. Recently this has been confirmed by Ley *et al.*[4] for amorphous Si and Ge using x-ray photoelectronic spectroscopy. These results are shown in Fig. 11. The fact that states are introduced in the valley between the two lower valence-band peaks in Figs. 9(a) and 10(a) for the

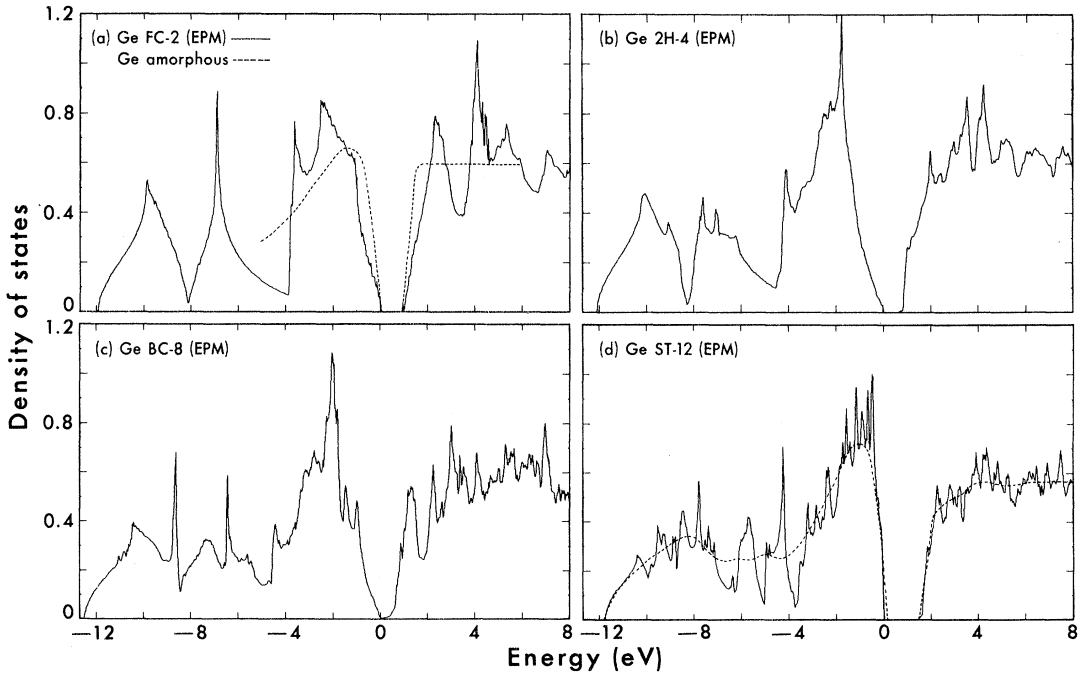

FIG. 9. Density of states of Ge in the (a) FC-2, (b) 2H-4, (c) BC-8, and (d) ST-12 structures using the EPM. The dotted line in (a) represents a sketch of the amorphous density of states obtained by Donovan *et al.* (Ref. 1). The dotted line in (d) represents the averaging of Bragg gaps for Ge ST-12 in this calculation.

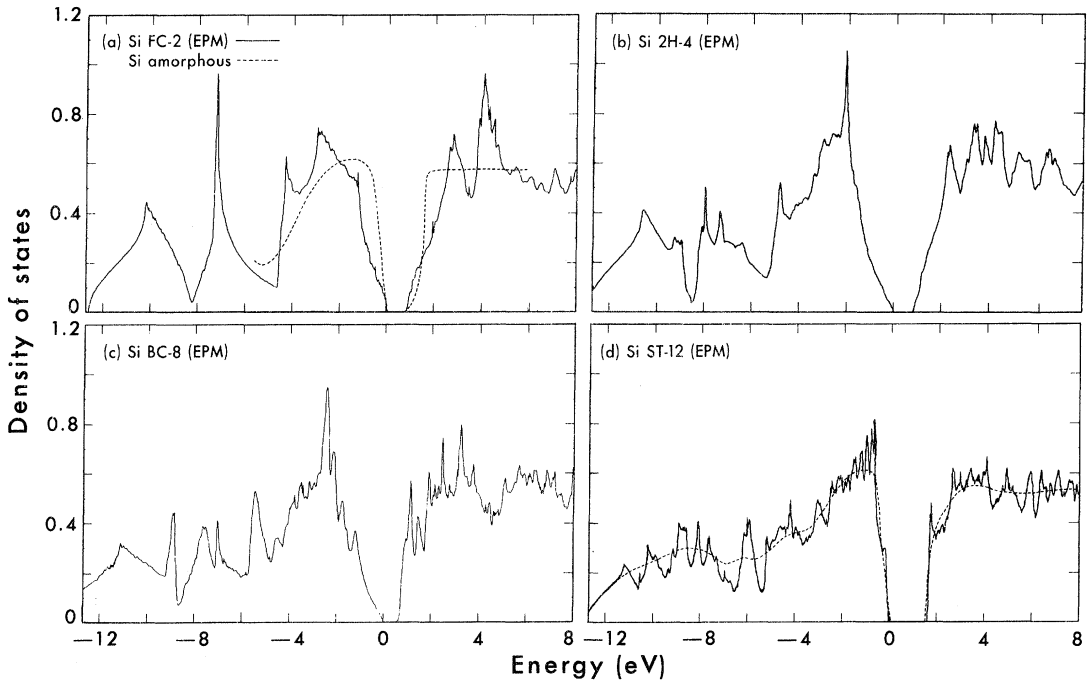

FIG. 10. Density of states of Si in the (a) FC-2, (b) 2H-4, (c) BC-8, and (d) ST-12 structures using the EPM. The dotted line in (a) represents a sketch of the amorphous density of states obtained by Pierce and Spicer (Ref. 2). The dotted line in (d) represents the averaging of Bragg gaps for Si ST-12 in this calculation.

amorphous and ST-12 phases, in such a way as to obtain a large hump where the valley used to be, can be primarily attributed to the presence of odd-numbered rings of bonds. This is suggested by the following simple argument. The FC-2 structure can be considered to be made up of six-numbered rings in the "chair" configuration. That is, we can pick a set of rings which can be brought together to make an FC-2 structure and we will assume for the moment that they do not lose their identity. Let us now isolate one of these rings and place one localized orbital at each of the atomic sites. We are thinking in terms of the one-state Hamiltonian mentioned earlier. The symmetry of this ring is D_{3d} and if we assume that these localized states transform into one another under D_{3d}, they then form a basis for the six-dimensional representation $\Gamma_6 = A_1 + E_1 + E_2 + B_1$. Thus we have six states consisting of two single states of symmetry A_1 and B_1, and two doubly degenerate states of symmetry E_1 and E_2. If we now assume only nearest-neighbor interactions H_I we obtain

$$E(A_1) = -2|H_I|, \quad E(E_1) = -|H_I|,$$

$$E(E_2) = |H_I|, \qquad E(B_1) = 2|H_I|.$$

Let us now isolate N rings at infinity. The density of states for this system is just an N-fold-degenerate single-ring density of states. As we bring these rings closer together, to make an FC-2 or 2H-4 structure, the rings will interact and the states are going to spread. Since we are considering only nearest-neighbor interactions we do not expect any drastic or significant differences when the inter-ring interaction becomes equal to the intra-ring interaction. For example, we can bring two rings together in such a way as to make a total of five rings. However, the energy spectrum for this system consists of just a splitting of each energy level of the two single-ring systems by about $|H_I|$. This is what we expected and thus the N-ring system should have a density of states which consists of two big humps and some type of valley in between. This density of states is then analogous to the two peaks at the bottom of the valence band in Figs. 9(a) and 10(a).

Consider now the same analysis with a five-numbered ring which we may take to have symmetry D_5. Assuming again that the localized states transform into each other under D_5, they span a five-dimensional representation $\Gamma_5 = A_1 + E_1 + E_2$. Thus we have five states consisting of a single state of symmetry A_1 and two doubly degenerate states of symmetry E_1 and E_2. We then obtain

$$E(A_1) = -2|H_I|, \quad E(E_1) = -2\cos\tfrac{2}{5}\pi\,|H_I|,$$

$$E(E_2) = -2\cos\tfrac{4}{5}\pi\,|H_I|.$$

The states of symmetry E_1 and E_2 lie intermediate in energy to those of the sixfold rings with symme-

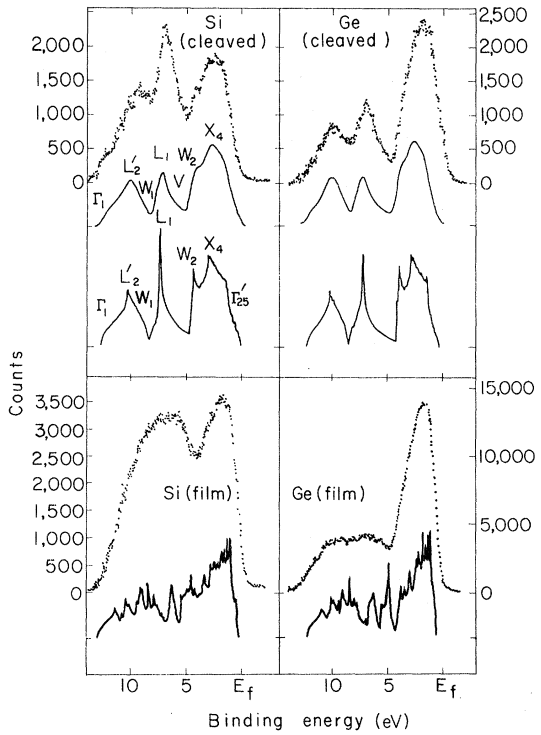

FIG. 11. Experimental x-ray photoelectron spectroscopy (XPS) results which are related to the density of states for Ge and Si in the FC-2 and amorphous phases. Top, experimental curves (dots) for Si and Ge in the FC-2 structure along with a sharp theoretical and a broadened theoretical (EPM) calculation. Bottom, XPS results for Si and Ge in the amorphous phase compared with the calculated density of states for Si and Ge in the ST-12 structure (EPM) from this work. The relative sizes of the humps in the Si experimental curves differ from those in Ge because of the differences in scattering cross sections of the $3s$, $3p$ and $4s$, $4p$ electrons.

try E_1, E_2, and B_1. Thus fivefold rings will introduce states in the valley between the two density-of-states peaks at the bottom of the valence band. In fact, the eigenvalues of any ring of order N are given by

$$E_n = -2|H_I| \cos(2n\pi/N), \quad n = 0, 1, \ldots, N-1. \tag{11}$$

Therefore sevenfold rings will also introduce states in the valley. Thus fivefold and sevenfold rings will help to produce a one-hump type of structure with a peak where the valley used to be. These results are consistent with those obtained by Weaire and Thorpe[19] for "Husumi cacti" made up of fivefold and sixfold rings.

The valence-band density-of-states edges of Ge and Si in the FC-2, 2H-4, and BC-8 structures (Figs. 9 and 10) are all similar in that they have gradual slopes. On the other hand, Ge and Si in the ST-12 and amorphous phases have very sharp edges. Along with this is the fact that there is a very noticeable shift of the hump at the top of the valence band to higher energies in the amorphous and ST-12 structures. We believe that the reason for this is an increase in the Coulomb-repulsion energy and kinetic energy because of variations in the bond angle in the amorphous and ST-12 phases. This can be shown by the following argument. Consider a system with a perfect tetrahedral arrangement of atoms like Ge FC-2, for example. The states in the large hump at the top of the valence band localize the electrons primarily in the bond whereas the states in the two large peaks at the bottom of the valence band localize the electrons primarily on the atoms. It is the electrons in the bonds which are more sensitive to changes in bond angle. Now the states at the high-energy side in the hump have a larger kinetic energy than the states at the lower-energy side in this hump. This reflects itself in the fact that the former states are very localized in the bonds whereas the latter states are more spread out in the bonds. Let us now consider an amorphous system and let us naively assume that we have just as many larger bond angles as smaller bond angles. Since the interaction between the bonds is not linear we will have an increase in the energy of each electronic state. However, the states at the lower-energy side in the large hump will have a larger overlap and a larger increase in energy than the states near the gap. This will produce an increase in the number of states near the gap and a steepening of the band edge. A simple calculation shows that the increase in the energy involved is of the same order as that observed in the amorphous case [Fig. 9(a)]. In the pseudopotential calculation for ST-12, Coulomb effects are not taken explicitly into account and the shifting of the peak is mainly due to an increase in the kinetic energy. We may argue in the same manner as above since variations in bond angles will produce a larger decrease in the effective volume occupied by the electrons at the lower-energy side of the hump than the electrons in states near the gap which are more localized in the bonds. This will result in an increase in the kinetic energy and we should obtain the same effect as in the amorphous case. This is evident in Fig. 9(d). Although the BC-8 structure has much smaller deviations in bond angles than ST-12 we can still notice an introduction of states near the gap when we compare BC-8 with 2H-4.

Finally, we would like to make some comparisons between our results for the BC-8 and ST-12 structures using the EPM and the Weaire model. If we compare ST-12 (Weaire) with Ge ST-12 (EPM) we notice a very good matching of gross structure. The δ function at -2 eV represents the large hump at the top of the valence band. The two strong

peaks near −4 eV and −6 eV are obtained in both cases and reveal a characteristic property of the structure. In Si ST-12 the peak at −4 eV has merged with the forward hump. In the BC-8 structure the comparisons are not as good. However, we still get a characteristic dip near −8 eV for both cases. The peak near −6 eV seems also to be well reproduced.

V. CONCLUSIONS

We have shown that long-range disorder is not necessary to reproduce the essential features of the amorphous data. By studying a series of structures that became more and more locally disordered we were able to draw some interesting conclusions as to what properties of the amorphous structure are important. We have found that deviations in bond angles will produce an enhancement of the states near the gap and what seems like a shift of the hump in the density of states at the top of the valence band to higher energies. The presence of local disorder also seems to smear out the strong structure in the region near the bottom of the conduction band. The presence of five- and seven-numbered rings will enhance the number of states in the valley between the two low-energy density-of-states peaks at the bottom of the valence band. The odd-numbered rings also have an effect in producing a "valence gap" and perhaps it is this feature that helps to retain the dip in the amorphous density of states shown in Fig. 11. Finally, the odd-numbered rings seem to have an effect on the size of the intrinsic energy gap. We found this to be a very large influence on the gap in the Weaire model. Now one may argue that this is of no realistic consequence since the conduction band in the Weaire model is inadequate and insufficient. Nevertheless, in the EPM calculation we find that the states near the gap at the bottom of the conduction band are s like and are rather localized. In this sense the predictions of the Weaire model may still be valid for these states. However, we are not implying that the presence of fivefold rings will produce an increase in the energy gap. As we found in our modified crystal the gap depends very critically on the Hamiltonian matrix elements. Furthermore, the amorphous phase is less dense and hence has probably fewer five-numbered rings than the ST-12 case. Therefore, this fact along with variations in the Hamiltonian matrix elements could produce a gap in the amorphous phase which is very nearly the same as that of FC-2.

We also believe that a microcrystallite model with 2H-4 microcrystallites is not substantiated by our calculations. This is clearly the case in the optical properties[22] even if we average the $\epsilon_2(\omega)$ function, since the peak lies higher in energy than the amorphous hump. This is also the case in the density of states for 2H-4 since an averaging does not reproduce in any way the amorphous features. One might suggest an amorphous structure made up of ST-12 microcrystallites and argue that small regions of microvoid structure could make up for bulk density differences. However, the radial distribution function for these structures would be quite different. The next-nearest neighbors in the Ge ST-12 structure at 3.45 and 3.64 Å would be hard to lose.

The random-network model seems like a reasonable model for the amorphous state. Its major problem is, of course, that of nonuniqueness. It is clearly obvious that one could make a random-network model and obtain a zero gap. Thus effects of stability must be very important in determining the particular types of random-network structure that can exist in a metastable state. The fact that amorphous samples are always prepared with very nearly the same gap clearly reflects this.

Finally, we hope this work will invite experimentalists to study the BC-8 and ST-12 structures which may have a variety of interesting applications. In particular, the ST-12 structure may have about 34 valleys in the conduction band. This feature in itself is interesting for several reasons. For example, it raises the question that ST-12 may be a superconducting semiconductor or that it may be a good host for the exciton droplet.

ACKNOWLEDGMENTS

We would like to thank L. Saravia and L. M. Falicov for some helpful suggestions. Part of this work was done under the auspices of the U. S. Atomic Energy Commission.

---

*Supported in part by the National Science Foundation under Grant Nos. GP 13632 and GH 35688.

[1]T. M. Donovan and W. E. Spicer, Phys. Rev. Lett. **21**, 1572 (1968); T. M. Donovan, W. E. Spicer, J. M. Bennett, and E. J. Ashley, Phys. Rev. B **2**, 397 (1970); T. M. Donovan, E. J. Ashley, and W. E. Spicer, Phys. Lett. A **32**, 85 (1970).

[2]D. T. Pierce and W. E. Spicer, Phys. Rev. B **5**, 3017 (1972).

[3]G. Wiech and E. Zöpf, in Proceedings of the International Conference on Band Structure Spectroscopy of Metals and Alloys, Glasgow, 1971 (unpublished).

[4]L. Ley, S. Kowalczyk, R. Pollak, and D. A. Shirley (unpublished).

[5]D. Weaire, Phys. Rev. Lett. **26**, 1541 (1971); D. Weaire and M. F. Thorpe, Phys. Rev. B **4**, 2508 (1971).

[6]T. C. McGill and J. Klima, Phys. Rev. B **5**, 1517 (1972).

[7]M. L. Rudee and A. Howie, Philos. Mag. **25**, 1001 (1972).

[8]J. S. Kasper and S. M. Richards, Acta Crystallogr. **17**, 752 (1964).

[9]M. L. Cohen and V. Heine, in *Solid State Physics*, edited by H. Ehrenreich, F. Seitz, and D. Turnbull (Academic, New York, 1970), Vol. 24, p. 37.

[10]C. H. Bates, F. Dachille, and R. Roy, Science **147**, 869 (1965). In this article Bates *et al.* incorrectly refer to Ge III

as a body-centered tetragonal structure.
[11]Short previews of our results are given in J. D. Joannopoulos and M. L. Cohen, Solid State Commun. **11**, 549 (1972); Phys. Lett. A **41**, 71 (1972); M. L. Cohen, in Proceedings of the Eleventh International Conference on the Physics of Semiconductors, Warsaw, 1972 (unpublished).
[12]R. H. Wentorf and J. S. Kasper, Science **139**, 338 (1963).
[13]M. L. Cohen and T. K. Bergstresser, Phys. Rev. **141**, 789 (1966).
[14]T. K. Bergstresser and M. L. Cohen, Phys. Rev. **164**, 1069 (1967).
[15]P. Löwdin, J. Chem. Phys. **19**, 1396 (1951).
[16]G. Gilat and L. J. Raubenheimer, Phys. Rev. **144**, 390 (1966).
[17]A. W. Luehrmann, thesis (University of Chicago, 1967) (unpublished).
[18]J. L. Birman, Phys. Rev. **115**, 1493 (1959).
[19]D. Weaire and M. F. Thorpe, in *Computational Methods for Large Molecules and Localiced States in Solids*, edited by F. Herman, A. D. McLean, and R. K. Nesbet (Plenum, New York, 1972).
[20]W. E. Spicer and T. M. Donovan, Phys. Lett. A **36**, 459 (1971).
[21]M. F. Thorpe and D. Weaire, Phys. Rev. Lett. **27**, 1581 (1971).
[22]J. D. Joannopoulos and M. L. Cohen (unpublished).

PHYSICAL REVIEW B VOLUME 7, NUMBER 6 15 MARCH 1973

Spin Correlations in a Magnetic Electron Gas

A. K. Rajagopal, J. Rath, and John C. Kimball
Department of Physics and Astronomy, Louisiana State University, Baton Rouge, Louisiana 70803
(Received 25 May 1972)

The density response function ($\chi_{\rho\rho}$), the longitudinal spin-correlation function (χ_{zz}), the transverse spin-correlation function (χ_{-+}), and the cross-correlation function ($\chi_{\rho z}$) involving the density and the z component of spin density are computed by employing two generalized moment-conserving (MC) schemes for a magnetic electron gas. The two schemes differ in their treatment of the one-electron states. These functions are also computed in the random-phase approximation (RPA) including exchange processes, in two different ways, by solving the resulting integral equations by a variational method due to one of the authors. We prove that in the absence of spin-orbit interactions, $\chi_{\rho z}(\vec{q}, \omega) = \chi_{z\rho}(\vec{q}, \omega)$, which enables us to set up a consistent MC scheme. In the paramagnetic state, only $\chi_{\rho\rho}$ and χ_{zz} are independent, and in the long-wavelength static limit they yield results in accordance with the RPA scheme. The plasma dispersion law for long wavelength is also found to be identical in the MC and RPA scheme. In the ferromagnetic case, one of the MC schemes gives the same results as the RPA results for the Stoner model, and very different results for the Coulomb gas. The long-wavelength spin-wave dispersion is found to be different in the two schemes. A new nonlocal-zero-moment-conserving scheme is set up which gives the same equations as the RPA. It is thus concluded that a local-MC scheme is different from the RPA by virtue of the actual structure of the correlation functions, even though in the paramagnetic limit the results are similar for the static long-wavelength limit.

I. INTRODUCTION

Some time ago, one of us (A.K.R.)[1] in collaboration with Brooks and Ranganathan, examined in some detail the various spin-correlation functions of the paramagnetic and ferromagnetic (unsaturated as well as fully saturated) interacting electron gas. These calculations were based on the random-phase approximation (RPA) and included *exchange contributions* for the appropriate vertex functions. One-electron energies were calculated in a Hartree–Fock (HF) scheme. Such a formalism, without the exchange contributions to the vertex functions, is known to be valid for high electron densities $r_s < 1$, of the paramagnetic state. (The density of the system is related to r_s by the condition that a sphere of radius r_s times the Bohr radius contains an average of one electron.) It is not yet clear that a formalism which includes these additional exchange processes will improve the validity of the RPA results without exchange for lower densities, which correspond to the electronic densities of alkali metals ($2 < r_s < 6$). The work presented here is in part an investigation of this question.

Attempts have been made previously to calculate the exchange effects for response and correlation functions. However, these calculations failed to satisfy both the "compressibility sum rule" and the condition that the pair-correlation function be positive. As pointed out in an article by Singwi *et al.*,[2] many of the calculations resulted in a negative pair-correlation function evaluated at the origin for densities corresponding to $r_s > 1$. Singwi *et al.*[2] originally proposed an ansatz which yielded positive or nearly positive pair correlations for $r_s \lesssim 6$, but the compressibility sum rule was badly violated for $r_s \gtrsim 3$. In a modification of their *Ansatz*, Singwi *et al.* obtained solutions yielding good agreement with the compressibility